$\bar{p}p$ ELASTIC SCATTERING AT 30 GeV/c INCIDENT MOMENTUM

Tom Fearnley
University College London , Dept. of Physics and Astronomy[1]

Annecy(LAPP) - CERN - Copenhagen(NBI) - Oslo - Genova - University College London Collaboration

ABSTRACT

The $\bar{p}p$ elastic differential cross-section at 30 GeV/c incident momentum has been measured in a two-arm spectrometer experiment (WA7) at the CERN SPS. The $|t|$-range covered extends from 0.5 to 5.0 $(GeV/c)^2$. A pronounced dip-bump structure is observed, with a sharp minimum around $|t| \approx 1.7$ $(GeV/c)^2$. The results are compared to existing $\bar{p}p$ data and to some model predictions.

---

[1] present address CERN, Geneva, Switzerland

1. Introduction

The p̄p elastic differential cross-section at 30 GeV/c incident beam momentum has been measured in the |t|-range 0.5 to 5.0 $(GeV/c)^2$. The experiment was part of a programme at the CERN SPS, in which hadron-proton elastic scattering has been measured over a wide range of momentum transfers and beam momenta[1-6], including p̄p 50 GeV/c scattering for $0.7<|t|<5.0$ $(GeV/c)^2$ [3]. This experiment is the first to measure p̄p 30 GeV/c elastic scattering.

2. The experiment

The experimental set-up, shown in Fig. 1, consisted of a double-arm spectrometer downstream of a liquid hydrogen target, upon which an unseparated high-intensity beam was incident. A differential Cerenkov counter (CEDAR1) in the beam line identified the incident antiprotons. The beam particles were detected by a beam hodoscope, while the scattered particles were detected by counter hodoscopes in the forward- and recoil-arm (H1,PR1 and H2,PR2). The scattered particle trajectories were determined by nine MWPCs (CH0-CH9). The momentum of the forward particles was measured by a spectrometer magnet with an integrated field of 1.8Tm. Particle identification in the forward arm was provided by two threshold Cerenkov counters (C1 and C2). The trigger imposed rough geometrical and kinematic constraints by means of hodoscope matrix correlations, beam signature requirements, and an energy threshold requirement for the forward particles, imposed by an iron/scintillator-sandwich calorimeter.

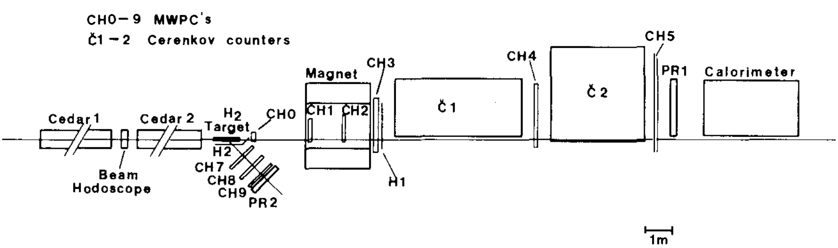

Figure 1: Schematic view of the WA7 experimental set-up.

Off-line track reconstruction and kinematic fitting is described in ref.2, together with the final event selection, based on minimum-χ^2 criteria, the background subtraction, and the various corrections applied.

3. Results

The $\bar{p}p$ 30 GeV/c elastic differential cross-section is shown in Fig.2a, together with the smoothed curve of the $\bar{p}p$ 50 GeV/c cross-section[3] (solid curve). A prominent dip around $|t| \approx 1.7\ (GeV/c)^2$ is observed at 30 GeV/c, as compared to the equally prominent dip at $|t| \approx 1.5\ (GeV/c)^2$ for $\bar{p}p$ 50 GeV/c. Our data thus show that the dip moves towards lower $|t|$-values as the energy increases.

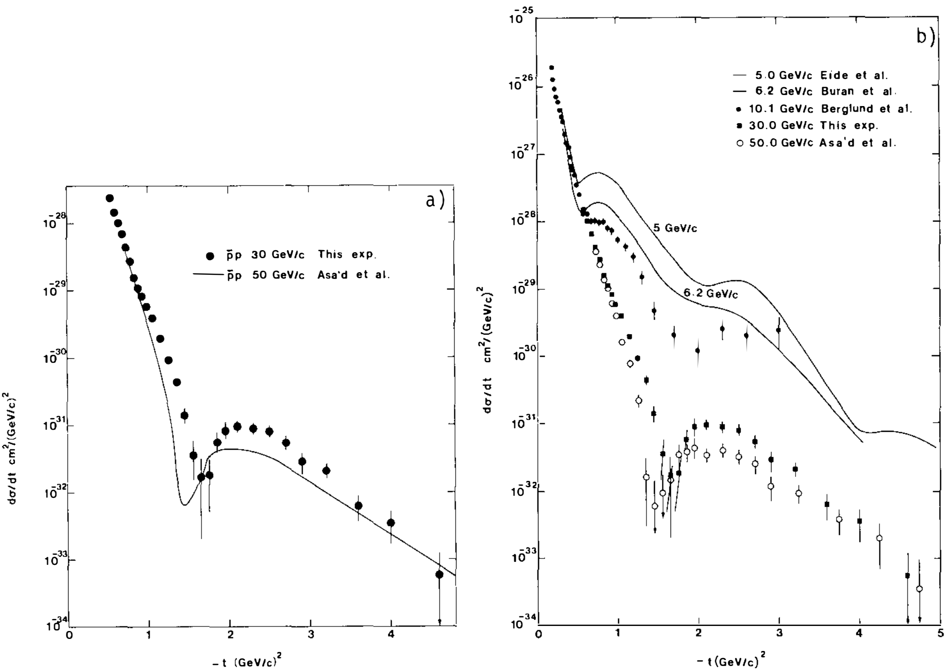

Figure 2: a) $\bar{p}p$ elastic differential cross-section at 30 GeV/c beam momentum (this exp.), compared with the smoothed curve of the $\bar{p}p$ 50 GeV/c cross-section of ref.3.

b) $\bar{p}p$ elastic differential cross-section at 30 GeV/c (this exp.) compared with $\bar{p}p$ data at 5.0[8], 6.2[9], 10.1[10] and 50[3] GeV/c. The data from refs. 8 and 9 are presented as smoothed curves.

This result disagrees with simple Geometrical Scaling (GS), which arrives at an outward dip movement in this energy region.[2] Kroll has pointed out that the energy may be too small to expect a simple GS behaviour, since the non-diffractive Regge-like component of the p̄p cross-section is appreciable at lower energies[7)]. Nevertheless, in ref.7 the p̄p 50 GeV/c cross-section is calculated from the pp 1480 GeV/c eikonal, and this is seen as evidence for GS at this energy. It is therefore surprising that GS seems to hold when applied at 50 GeV/c, while apparently the p̄p 30 GeV/c cross-section cannot be reproduced.

Fig.2b[3,8-10)] shows that the structure around $|t|\approx 0.5$ (GeV/c)² in low-energy p̄p cross-sections has disappeared in the 30 and 50 GeV/c data, although a change of slope is still apparent at $|t|\approx 0.8$ (GeV/c)² in the 30 GeV/c data. Moreover, the inward dip movement naturally associates the prominent dip in the 30 and 50 GeV/c data with the structure around $|t|\approx 2$ (GeV/c)² seen at 10 GeV/c[10)].

Such a dip development is in sharp disagreement with predictions by the geometrical model of Chou and Yang[11)], in which the dip at 50 GeV/c is associated with the low-$|t|$ structure at lower energies, interpreted as the first diffractive minimum. In accordance with the consequent outward dip movement, a dip at $|t|\approx 1.1$ (GeV/c)² is explicitely predicted for p̄p 30 GeV/c. Fig.3 (from ref.11) shows the predicted pp and p̄p dip movement as a function of total cross-section. The curves I-IV represent the first, second and higher order dips predicted. Some experimental data points are plotted, including the p̄p 50 GeV/c dip position. The experimental p̄p 30 GeV/c dip position has been added to the figure, together with the p̄p 10 GeV/c data point for the structure around $|t|\approx 2$ (GeV/c)². Associating the 30 and 50 GeV/c dip with the 10 GeV/c structure, a dip movement contrary to the Chou-Yang prediction is obtained (dotted line).

The nucleon core model of Islam and Guillaud[12)] correctly associates the dip at 50 GeV/c with the low-energy structure around $|t|\approx 2$ (GeV/c)², seen as the second destructive interference between a diffractive and a hard amplitude. The model thus predicts the observed inward dip movement. The p̄p 50 GeV/c cross-section is reproduced by fitting a set of eight diffractive and hard scattering parameters[12)]. A similar analysis of the 30 GeV/c data will reportedly be done to further test the model.

---

[2] GS predicts a dip movement according to $-t_{dip}\sim 1/\sigma_{tot}$. Since σ_{tot} decreases between 30 and 50 GeV/c, GS leads to an outward dipmovement with increasing energy.

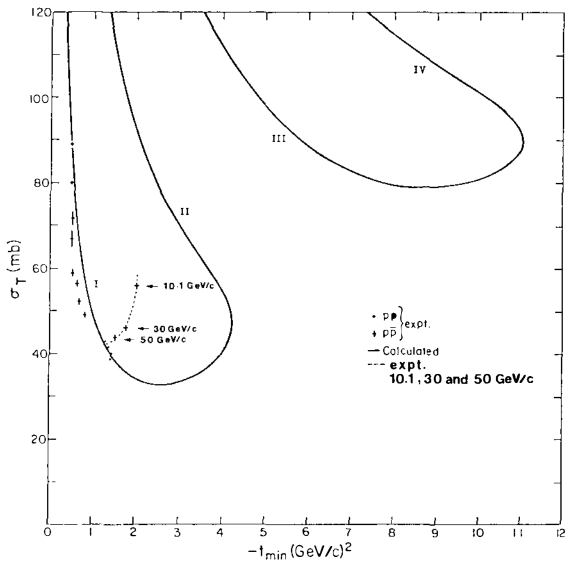

Figure 3: pp and p̄p dip movement as a function of total cross-section, predicted in the Chou-Yang model (figure from ref.11). Some experimental data points are plotted. The curves I-IV represent the multiple dips predicted. The experimental p̄p 10 and 30 GeV/c data points have been added by the author. Dotted line is obtained by associating the 30 and 50 GeV/c dip with the 10 GeV/c structure at $|t|\approx 2$ (GeV/c)².

A recent QCD model involving triple gluon exchange is reported to reproduce the p̄p 50 GeV/c cross-section well[13]. We are eagerly awaiting model predictions for the p̄p 30 GeV/c cross-section.

Recent FNAL p̄p data at 100 and 200 GeV/c[14] indicate that the dip at $|t|\approx 1.5$ (GeV/c)² persists to at least 100 GeV/c incident momentum and that the 200 GeV/ data are consistent with the same behaviour, although statistics are poor. Hence, little movement of the dip is seen between 50 and 200 GeV/c.

Fig.4a shows that the p̄p 50 GeV/c cross-section[3] almost coincides with ISR pp data at 1064 GeV/c[15]. Moreover, in recent WA7 data[6] the pp 50 GeV/c cross-section features only a shoulder. It is possible that this difference in pp and p̄p behaviour reflects the larger real part of the pp amplitude at lower energies, effectively filling in the pp dip ($\rho_{pp}\approx -0.2$ at 50 GeV/c[16]). At intermediate energies, ρ_{pp} approaches $\rho_{\bar{p}p}\approx 0$, and a pp dip starts developing

(p_{lab} >≈100 GeV/c[14]). At collider energies, both ρ_{pp} and $\rho_{\bar{p}p}$ seem to be non-negligible, and, in fact, recent UA4 p̄p data at $\sqrt{s}$=540 GeV for $|t|<1.5$ (GeV/c)² show no dip structure[17].

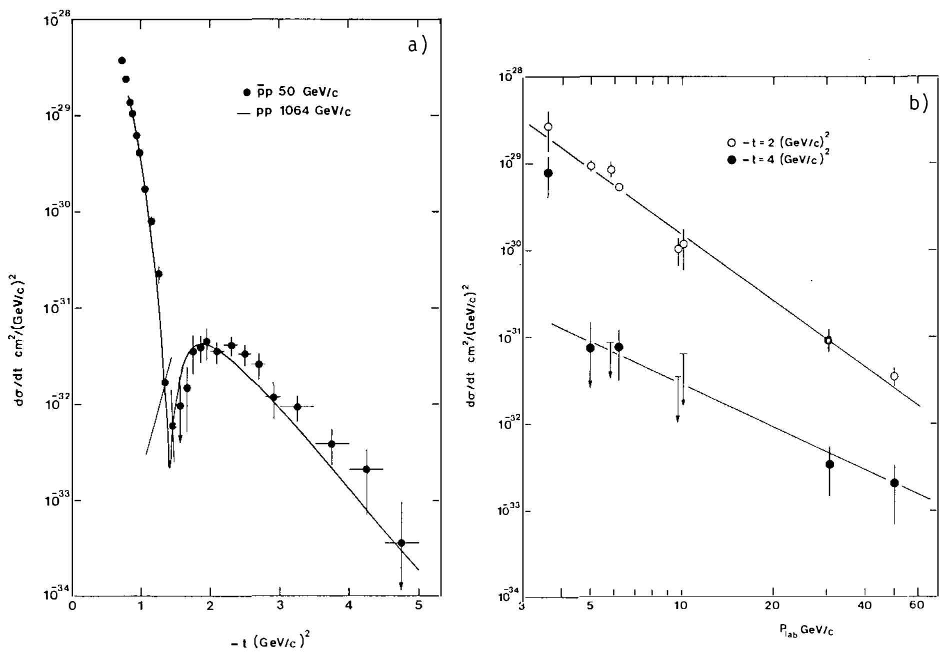

Figure 4: a) p̄p elastic differential cross-section at 50 GeV/c[3], compared with the smoothed ISR pp 1064 GeV/c cross-section[15].

b) Energy dependence of p̄p elastic differential cross-section at fixed |t|-values of 2.0 and 4.0 (GeV/c)². The straight lines are eye-fits through data points at 3.6 GeV/c[18], 5.0 GeV/c[8], 5.8 GeV/c[19], 6.2 GeV/c[9], 9.7 GeV/c[19], 10.1 GeV/c[10], 30 GeV/c (this exp.) and 50 GeV/c[3].

The energy dependence of the p̄p elastic cross-section at fixed |t|-values of 2.0 and 4.0 (GeV/c)² is shown in Fig.4b[3,8-10,18,19]. Parametrizing as

$$d\sigma/dt \sim p_{lab}^{-\alpha} ,$$

we find $\alpha \simeq 2.5$ for $|t|=2$ (GeV/c)², and $\alpha \simeq 1.6$ for $|t|=4$ (GeV/C)². This energy dependence differs from what we find for pp scattering in the same energy range[6], where $\alpha_{pp}(t)$ is found to increase roughly linearly with |t| according to $\alpha_{pp}(t) \approx 0.6|t|+0.7$.

References

1) R. Almas et al., Phys.Lett.93B (1980) 199.
2) C. Baglin et al., Preprint CERN-EP/82-155 (1982)
(to be published in Nucl.Phys.B).
3) Z. Asa'd et al., Phys.Lett.108B (1982) 51.
4) Z. Asa'd et al., Phys.Lett.118B (1982) 442.
5) Z. Asa'd et al., Phys.Lett.123B (1983) 265.
6) Z. Asa'd et al. pp elastic scattering at 50 GeV/c incident momentum.
(to be published in Phys.Lett.B).
7) P. Kroll, Z.Phys.C15 (1982) 67.
8) A. Eide et al., Nucl.Phys.B60 (1973) 173.
9) T. Buran et al., Nucl.Phys.B97 (1975) 11.
10) A. Berglund et al., Nucl.Phys.B176 (1980) 346.
11) T.T. Chou and C.N. Yang, Phys.Rev.Lett.46 (1981) 764.
12) M.M. Islam and J.P. Guillaud, University of Connecticut Preprint
80-0861 (1980).
13) P.V. Landshoff. Contribution to the Workshop on SPS Fixed-Target
Physics, CERN Dec.1982, and these Proceedings.
14) D.H. Kaplan et al., FNAL Report, Fermilab-Pub-82/40-EXP 7120.577.
15) E. Nagy et al., Nucl.Phys.B150 (1979) 221.
16) K. Runge, Proc. Int. Conf. on HEP, EPS Lisbon 1981, p.328.
17) J. Timmermand. UA4 results presented at this Moriond Conference.
18) W.M. Katz, B. Forman and T. Ferbel, Phys.Rev.Lett.19 (1967) 265.
19) D.P. Owen et al., Phys.Rev.181 (1969) 1794.